Dynamics of PDE, Vol.19, No.4, 247-271, 2022

Dynamic analysis of a diffusive eco-epidemiological system with fear effect and prey refuge

Tingting Ma and Xinzhu Meng

Communicated by Y. Charles Li, received May 7, 2022.

Abstract. In the evolutionary development of species, the prey can produce the fear effect in the face of predation behaviors. This fear effect may affect the own reproduction growth of the prey. In order to reduce the risk of predation, the prey has the instinct to protect themselves. At the same time, the population is easy vulnerable by disease in the ecosystem. Driven by these biological facts, we propose an eco-epidemiological system with two-predator-one-prey that considers fear effect and prey refuge. At the same time, we consider the impact of spatial diffusion on the stability of the system. We discuss the conditions for the existence of all equilibrium points with biological meanings in non-spatial system. We also obtain local stability conditions for all equilibrium points. We show that the deterministic system is bistable. Kolmogorov analysis is used to analyze the appearance of limit cycles and chaos in the non-spatial system. We consider k as a bifurcation parameter and study the existence of Hopf bifurcation. In the spacial diffusion system, we deduce the local stability conditions of the diffusion system and obtain the occurrence conditions of Turing instability. Numerical simulations are given to explain the phenomena beyond the scope of analytical methods and better understand the complex predator-prey interactions.

Contents

1991 *Mathematics Subject Classification.* Primary 37G15 92B05; Secondary 18F25 92D30.

Key words and phrases. Eco-epidemiological system, Fear effect, Bi-stability, Hopf bifurcation, Turing instability.

Corresponding author: Xinzhu Meng. Email: mxz721106@sdust.edu.cn (XZ Meng), ttmsdust17@163.com (TT Ma).

©2022 International Press

1. Introduction

Ecological epidemiology, as a branch of mathematical ecology, has aroused extensive research. When we study the predator-prey system, we can find rich dynamic behaviors between predator and prey. In addition, the predator is similar to the prey, and it can also be affected by natural factors, the most common of which is the disease. In a certain ecological environment, the spread of infectious diseases and the interaction between species can not be ignored, so it is essential to observe the dynamics of the environmental interaction between species and infectious diseases. Based on the classic SIR epidemic model, we take the predation behavior of animals into account, it can be found that when a predator is infected with a disease, it will lose its predation ability and then reduce its predation efficiency by infecting susceptible predators. Diseases can spread from predator to predator, so it is vital to study predator-predator systems, especially infections in predator populations. Many scholars are attracted to the study of ecological populations [**1**–**5**]. Feng et al. [**6**] proposed a stochastic ecological population model and discussed the effects of white noise on stability of three populations. So we consider a three-species ecosystem, where one predator is infected and not able to eat any prey, and the other predator is susceptible and has ability to catch the prey. From several classical predator-prey systems, we can find authors usually considered the consumption of the prey as a result of direct killing by predators or natural death [**13**–**16**]. In 1990 Steven Lima and Lawrence Dill published a review paper at Simon Fraser University in British Columbia, Canada, they explored the possibility that the effects of predators may go beyond directly killing prey which led some biologists to recognize that the non-lethality of predatory behavior (the fear effect) has been underestimated. In recent years, biologists have been simulated the behavior of vertebrates on land [**7**–**10**], and we have found that the fear effect of prey reduces reproduction to some extent according to their studies, which means that in nature, the abundance of the prey is determined not only by its birth rate, death rate and direct predation but also by the fear effect of predator [**11**], authors showed that high levels of fear could make the predator-prey system be stable while low levels of fear can induce multiple limit cycles. In [**12**], we know the fear effect can induce stability in the system.

As the prey evolved, they came up with a number of ways to protect themselves from predators, the most common of which was to build prey refuge. A spatial prey refuge protects a certain percentage of prey from predation. The emergence of prey refuge can provide prey with a degree of protection and reduce the chance of extinction. The study of prey refuge has become a topic of interest for some scholars [**17**–**20**]. Collings in [**21**] proposed a prey-predator system with prey refuge, and he found the increasing of refuge made a population outbreaks. In [**22**], the authors considered a predator-prey model with constant-rate prey harvesting and prey refuge, they obtained the result that prey refuge may affect the harvesting efforts of the prey. Based on the above factors, we establish the following model.

For the prey-predator system, many researchers studied logistic prey growth, we take into account the effect of fear on the prey growth. In 1959, Holling proposed the

predator-prey model by using Holling II functional response in [**23**]. In this paper, we consider the prey refuge as a Holling II functional response which is written as

$$\frac{x}{1+a(1-m)x}.$$

Then we consider the following equation:

$$\begin{cases} \frac{\mathrm{d}X}{\mathrm{d}t} = X\left[\frac{r}{1+kS} - \alpha X - \frac{\beta(1-m)S}{1+a(1-m)X}\right], \\ \frac{\mathrm{d}S}{\mathrm{d}t} = S\left[\frac{\beta_1(1-m)X}{1+a(1-m)X} - \delta_1 - cI\right], \\ \frac{\mathrm{d}I}{\mathrm{d}t} = I(cS - \delta_2), \end{cases} \tag{1.1}$$

where X, S, I represent the density of prey, susceptible predator and infected predator at time t, respectively. Moreover, another functional response can be defined as

$$\frac{mx^2}{a+x^2}$$

which is known as Holling III functional response. We apply the non-monotonic functional response to the rate of transmission between infected predator and susceptible predator which we suggest that susceptible predators have a sense of self-protection against infected predators. Based on the system (1.1), we propose the modified model

$$\begin{cases} \frac{\mathrm{d}X}{\mathrm{d}t} = X\left[\frac{r}{1+kS} - \alpha X - \frac{\beta(1-m)S}{1+a_1(1-m)X}\right], \\ \frac{\mathrm{d}S}{\mathrm{d}t} = S\left[\frac{\beta_1(1-m)X}{1+a_1(1-m)X} - \delta_1 - \frac{cI}{bS^2+a_2}\right], \\ \frac{\mathrm{d}I}{\mathrm{d}t} = I\left[\frac{cS}{bS^2+a_2} - \delta_2\right], \end{cases} \tag{1.2}$$

$(1-m)X$ is the number of prey available to the predator, where $m \in [0,1)$. It is well known that in real ecosystems, the development and interaction of species depend on the spatial environment, many researchers are concerned with the dynamics of spatially uniform steady-state solutions of diffusion systems. Motivated by the pioneer works, the reaction-diffusion predator-prey system is of the form:

$$\begin{cases} \frac{\partial X}{\partial t} = d_1 \triangle X + X\left[\frac{r}{1+kS} - \alpha X - \frac{\beta(1-m)S}{1+a_1(1-m)X}\right], & x \in \Omega, t > 0, \\ \frac{\partial S}{\partial t} = d_2 \triangle S + S\left[\frac{\beta_1(1-m)X}{1+a_1(1-m)X} - \delta_1 - \frac{cI}{bS^2+a_2}\right], & x \in \Omega, t > 0, \\ \frac{\partial I}{\partial t} = d_3 \triangle I + I\left[\frac{cS}{bS^2+a_2} - \delta_2\right], & x \in \Omega, t > 0, \\ \frac{\partial X}{\partial \nu} = \frac{\partial S}{\partial \nu} = \frac{\partial I}{\partial \nu} = 0, & x \in \partial\Omega, t > 0, \\ X(x,0) = S(x,0) = I(x,0) = 0, & x \in \Omega, t > 0, \end{cases} \tag{1.3}$$

where ν is the normal outward vector of $\partial\Omega$, Δ is Laplacian operator, Ω is a bounded open region with smooth boundaries $\partial\Omega$, and the system is under the Neumann boundary value conditions, and other parameters are explained in Table 1. The aim of this paper is to investigate the influence of prey refuge and fear effect on the stability of the system (1.3). The organization of this paper is as follows: In Section 1, we present a formulation of a new class of eco-epidemiological system, and mathematically analyze the non-spatial system (1.2). We prove the boundedness of solutions, and obtain the conditions under which all equilibrium points exist are given in Section 2. In Section 3, we analyze the conditions of stability around equilibrium points. Kolmogorov analysis is applied to examine appearance of limit cycle and chaos in non-spatial system (1.2). In Section 4, the local stability and Turing instability for spatio-temporal system (1.3) have been discussed. Numerical

Parameter	Meaning	value	source
r	Intrinsic growth rate of prey	0.45	Assumed
k	The level of fear effect	0.6	[**25**]
α	Intra-specific competition rate	0.18	Assumed
β	Catching rate	0.9	[**26**]
β_1	The effective catching rate	0.5	Assumed
m	The level of the prey refuge	0.25	[**25**]
a_1	Saturation constant of prey	0.75	Assumed
a_2	Saturation constant of susceptible predator	0.8	Assumed
b	Inverse measure of inhibitory effect of infected predator	0.4	[**28**]
δ_1	The death rate of the susceptible predator	0.18	[**27**]
δ_2	The death rate of the infected predator	0.22	[**27**]
c	The infectious rate	0.5	[**24**]

TABLE 1. Parameters and their meanings

simulations of spatial as well as non-spatial system are presented to verify the correctness of the theoretical results in Section 5. Finally, we present conclusions of this paper in Section 6.

2. Properties of the corresponding temporal system (1.2)

In this section, we mainly discuss some properties of system (1.2), including the boundedness of solutions, the meanings of equilibrium points, and the conditions where equilibrium points exist.

2.1. Boundedness. In an ecosystem, the solution with biological significance must be nonnegative and bounded, thus we give the following theorem.

THEOREM 2.1. *For any positive initial value $X(0) = X_0 > 0$, $S(0) = S_0 > 0$, $I(0) = I_0 > 0$. It is clear that all positive solutions of the system (1.2) which initiate in $\mathbb{R}^3_+$ are bounded.*

PROOF. From the first equation of system (1.2), one has

$$\begin{aligned} \frac{\mathrm{d}X}{\mathrm{d}t} &= \frac{rX}{1+kS} - \alpha X^2 - \frac{\beta(1-m)SX}{1+a_1(1-m)X} \\ &\leq rX - \alpha X^2 = X(r-\alpha X), \end{aligned}$$

which means $X \leq \frac{r}{\alpha}$.
Denote the positive definite function

$$V = \frac{\beta_1}{\beta}X + S + I. \tag{2.1}$$

Differentiating both sides of the equation (2.1) along time t, one yields,

$$\begin{aligned}
\frac{\mathrm{d}V}{\mathrm{d}t} &= \frac{\beta_1}{\beta}\frac{\mathrm{d}X}{\mathrm{d}t} + \frac{\mathrm{d}S}{\mathrm{d}t} + \frac{\mathrm{d}I}{\mathrm{d}t} \\
&= \frac{\beta_1 X}{\beta}\left[\frac{r}{1+kS} - \alpha X - \frac{\beta(1-m)S}{1+a_1(1-m)X}\right] \\
&\quad + S\left[\frac{\beta_1(1-m)X}{1+a_1(1-m)X} - \delta_1 - \frac{cI}{bS^2+a_2}\right] + I\left[\frac{cS}{bS^2+a_2} - \delta_2\right] \\
&= \frac{\beta_1 r X}{(1+kS)\beta} - \frac{\beta_1\alpha}{\beta}X^2 - \delta_1 S - \delta_2 I \\
&\leq \frac{\beta_1 r^2}{\beta\alpha} + \frac{\beta_1 r}{\beta\alpha} - \left(\frac{\beta_1 X}{\beta} + \delta_1 S + \delta_2 I\right) \\
&= \frac{\beta_1 r(r+1)}{\beta\alpha} - \left(\frac{\beta_1 X}{\beta} + \delta_1 S + \delta_2 I\right) \\
&\leq \frac{\beta_1 r(r+1)}{\beta\alpha} - P\left(\frac{\beta_1}{\beta}X + S + I\right) \\
&= \frac{\beta_1 r(r+1)}{\beta\alpha} - PV,
\end{aligned}$$

where $P = \min\{1, \delta_1, \delta_2\}$. Therefore, all positive solutions in system (1.2) are uniformly bounded for all $t \geq 0$, and confined in the following region $(X, S, I) \in R_+^3$: $0 \leq X \leq \frac{\beta}{\alpha}, \frac{\beta_1}{\beta}X + S + I \leq \frac{\beta_1 r(r+1)}{\beta\alpha}$. This completes the proof. □

2.2. Equilibria points. In this subsection, we analyze the related properties of equilibrium points. We first show equilibrium points of the system (1.2) which are expressed as follows.

1. The trivial equilibrium point $E_0 = (0, 0, 0)$ always exists, and it is not stable.

2. The equilibrium point $E_1 = (\frac{r}{\alpha}, 0, 0)$ always exists, as the prey population grows to a fixed value in the absence of predation.

3. Due to the extinction scenario of susceptible predator, the infected predator population can not be existed, so there is no equilibrium point in the $x - z$ plane. Moreover, neither susceptible predator population, nor infected predator population can survive in the absence of prey species X, hence there is no equilibrium point in the $y - z$ plane.

3. In the absence of infected predator, the susceptible predator can survive on its prey. Hence the equilibrium point $E_2 = (\bar{X}, \bar{S}, 0)$ exists in the interior of positive quadrant of $x - y$ plane.

4. The positive equilibrium point $E_* = (X_*, S_*, I_*)$ exists, if and only if there is a positive solution to the following algebraic nonlinear system.

Next, we will give a detailed expression of the equilibrium points. By setting the right-hand side equal zero, it is easy to get the trivial equilibrium point $E_0 = (0, 0, 0)$ and prey-only equilibrium point $E_1 = (\frac{r}{\alpha}, 0, 0)$.

For the biological significance equilibrium points E_2, we have

$$\begin{cases} \bar{X}\left[\frac{r}{1+k\bar{S}} - \alpha\bar{X} - \frac{\beta(1-m)\bar{S}}{1+a_1(1-m)\bar{X}}\right] = 0, \\ \bar{S}\left[\frac{\beta_1(1-m)\bar{X}}{1+a_1(1-m)\bar{X}} - \delta_1\right] = 0, \end{cases} \tag{2.2}$$

from the second equation, we have $\bar{X} = \frac{\delta_1}{(\beta - a_1\delta_1)(1-m)}$, which means $\beta - a_1\delta_1 > 0$. Then putting $\bar{X}$ in the first equation of (2.2), we have

$$\begin{aligned} & \frac{r}{1+k\bar{S}} - \alpha\bar{X} - \frac{\beta(1-m)\bar{S}}{1+a_1(1-m)\bar{X}} \\ = \; & r + a_1 r(1-m)\bar{X} - [\alpha\bar{X} + a_1\alpha(1-m)\bar{X}^2](1+k\bar{S}) - \beta(1-m)(1+k\bar{S})\bar{S} \\ = \; & -k\beta(1-m)\bar{S}^2 - [\alpha k\bar{X} + a_1\alpha k(1-m)\bar{X}^2 + \beta(1-m)]\bar{S} + r + a_1 r(1-m)\bar{X} \\ & -\alpha\bar{X} - a_1\alpha(1-m)\bar{X}^2 = 0, \end{aligned}$$

let $A = -k\beta(1-m)$, $B = -\left(\alpha k\bar{X} + a_1\alpha k(1-m)\bar{X}^2 + \beta(1-m)\right)$, $C = r + a_1 r(1-m)\bar{X} - \alpha\bar{X} - a_1\alpha(1-m)\bar{X}^2$. This is a quadratic polynomial with respect to $\bar{S}$, and there is a unique positive solution $\bar{S} = \frac{-B+\sqrt{B^2-4AC}}{2A}$ if and only if $C > 0$.
For E_*, let both size of the equation (1.2) equal zero, we get

$$\begin{cases} X_*\left[\frac{r}{1+kS_*} - \alpha X_* - \frac{\beta(1-m)S_*}{1+a_1(1-m)X_*}\right] = 0, \\ S_*\left[\frac{\beta_1(1-m)X_*}{1+a_1(1-m)X_*} - \delta_1 - \frac{cI_*}{bS_*^2+a_2}\right] = 0, \\ I_*\left[\frac{cS_*}{bS_*^2+a_2} - \delta_2\right] = 0, \end{cases} \tag{2.3}$$

from the last equation in (2.3), we have $S_1 = \frac{c-\sqrt{c^2-4ba_2\delta_2^2}}{2b\delta_2}$, $S_2 = \frac{c+\sqrt{c^2-4ba_2\delta_2^2}}{2b\delta_2}$, if $c^2 - 4ba_2\delta_2^2 > 0$. From the first equation, X_* can be calculated as

$$\begin{aligned} 0 \; = \; & [-a_1\alpha(1-m) - a_1\alpha k(1-m)S_*]X_*^2 \\ & +[-\alpha - \alpha kS_* + a_1 r(1-m)]X_* - k\beta(1-m)S_*^2 - \beta(1-m)S_* + r. \end{aligned} \tag{2.4}$$

From the quadratic equation, we can make the following classification:

Case i: $C_1 > 0$, then the quadratic equation (2.4) has one positive solution $X_1 = \frac{-B_1-\sqrt{B_1^2-4A_1C_1}}{2A_1}$,

Case ii: $C_1 < 0$, $B_1 > 0$ and $B_1^2 - 4A_1C_1 > 0$, the quadratic equation (2.4) has two positive solutions

$$X_1 = \frac{-B_1 - \sqrt{B_1^2 - 4A_1C_1}}{2A_1}, \quad X_2 = \frac{-B_1 + \sqrt{B_1^2 - 4A_1C_1}}{2A_1},$$

where

$$\begin{aligned} A_1 &= -a_1\alpha(1-m) - a_1\alpha k(1-m)S_*, \\ B_1 &= -\alpha - \alpha kS_* + a_1 r(1-m), \\ C_1 &= -k\beta(1-m)S_*^2 - \beta(1-m)S_* + r. \end{aligned}$$

Putting S_* and X_* into the second equation of (2.3), we have

$$I_* = \frac{bS_*^2 + a_2}{c}\left(\frac{\beta_1(1-m)X_*}{1+a_1(1-m)X_*} - \delta_1\right).$$

Next, we show the analysis of stability of system (1.2) around different equilibrium points.

3. Stability of system (1.2)

In this subsection, we linearise the system (1.2) near the equilibrium points to analyze the local stability of all biological feasible states, we first define

$$\begin{cases} \frac{r}{1+kS} - \alpha X - \frac{\beta(1-m)S}{1+a_1(1-m)X} = M_1, \\ \frac{\beta_1(1-m)X}{1+a_1(1-m)X} - \delta_1 - \frac{cI}{bS^2+a_2} = M_2, \\ \frac{cS}{bS^2+a_2} - \delta_2 = M_3. \end{cases}$$

The variational matrix V of system (1.2) is obtained as

$$V = \begin{pmatrix} X\frac{\partial M_1}{\partial X} + M_1 & X\frac{\partial M_1}{\partial S} & X\frac{\partial M_1}{\partial I} \\ S\frac{\partial M_2}{\partial X} & S\frac{\partial M_2}{\partial S} + M_2 & S\frac{\partial M_1}{\partial I} \\ I\frac{\partial M_3}{\partial X} & I\frac{\partial M_3}{\partial S} & I\frac{\partial M_3}{\partial I} + M_3 \end{pmatrix}. \tag{3.1}$$

The variational matrix around $E_0 = (0, 0, 0)$ can be expressed as

$$V_{E_0} = \begin{pmatrix} r & 0 & 0 \\ 0 & -\delta_1 & 0 \\ 0 & 0 & -\delta_2 \end{pmatrix}.$$

The extinction equilibrium point $E_0 = (0, 0, 0)$ is unstable saddle point, indeed, V_{E_0} has one positive eigenvalue r. Hence, V_{E_0} is one dimensional unstable.

The variational matrix around $E_1 = (\frac{r}{\alpha}, 0, 0)$ can be written as

$$V_{E_1} = \begin{pmatrix} -r & -\frac{kr^2}{\alpha} - \frac{r\beta(1-m)}{\alpha+a_1r(1-m)} & 0 \\ 0 & \frac{r\beta_1(1-m)}{\alpha+a_1r(1-m)} - \delta_1 & 0 \\ 0 & 0 & -\delta_2 \end{pmatrix}.$$

Obviously, the equilibrium point $E_1 = (\frac{r}{\alpha}, 0, 0)$ has one negative eigenvalue $-\delta_2$, another two eigenvalues of variational matrix V_{E_1} can be analyzed by discussing the following variational matrix

$$V_2 = \begin{pmatrix} -r & -\frac{kr^2}{\alpha} - \frac{r\beta(1-m)}{\alpha+a_1r(1-m)} \\ 0 & \frac{r\beta_1(1-m)}{\alpha+a_1r(1-m)} - \delta_1 \end{pmatrix},$$

$$\mathtt{tr}(V_2) = -r + \frac{r\beta_1(1-m)}{\alpha + a_1r(1-m)} - \delta_1, \ \mathtt{det}(V_2) = -r\left(\frac{r\beta_1(1-m)}{\alpha + a_1r(1-m)} - \delta_1\right),$$

if $\frac{r\beta_1(1-m)}{\alpha+a_1r(1-m)} - \delta_1 < 0$, the eigenvalues of V_2 have negative real part, which means V_{E_1} has three negative eigenvalues. Hence E_1 is locally asymptotically stable when $\frac{r\beta_1(1-m)}{\alpha+a_1r(1-m)} - \delta_1 < 0$ holds.

The variational matrix around $E_2 = (\bar{X}, \bar{S}, 0)$ is

$$V_{E_2} = \begin{pmatrix} \frac{r}{1+k\bar{S}} - 2\alpha\bar{X} - \frac{\beta(1-m)\bar{S}}{(1+a_1(1-m)\bar{X})^2} & -\frac{kr\bar{X}}{(1+k\bar{S})^2} - \frac{\beta(1-m)\bar{X}}{1+a(1-m)\bar{X}} & 0 \\ \frac{\beta_1(1-m)\bar{S}}{(1+a_1(1-m)\bar{X})^2} & 0 & \frac{c\bar{S}}{b\bar{S}^2+a_2} \\ 0 & 0 & \frac{c\bar{S}}{b\bar{S}^2+a_2} - \delta_2 \end{pmatrix}.$$

The variational matrix V_{E_2} has an eigenvalue $\frac{c\bar{S}}{b\bar{S}^2+a_2} - \delta_2$, if $\frac{c\bar{S}}{b\bar{S}^2+a_2} - \delta_2 > 0$, the E_2 is always unstable. Otherwise, we analyze the following variational matrix

$$V_3 = \begin{pmatrix} \frac{r}{1+k\bar{S}} - 2\alpha\bar{X} - \frac{\beta(1-m)\bar{S}}{(1+a(1-m)\bar{X})^2} & -\frac{kr\bar{X}}{(1+k\bar{S})^2} - \frac{\beta(1-m)\bar{X}}{1+a(1-m)\bar{X}} \\ \frac{\beta_1(1-m)\bar{S}}{(1+a(1-m)\bar{X})^2} & 0 \end{pmatrix}.$$

By a simple calculation, we obtain that all eigenvalues have negative real part if and only if

$$\frac{r}{1+k\bar{S}} - 2\alpha\bar{X} - \frac{\beta(1-m)\bar{S}}{[1+a(1-m)\bar{X}]^2} < 0.$$

The variational matrix at the positive equilibrium $E_* = (X_*, S_*, I_*)$ is given by

$$V_{E_*} = \begin{pmatrix} a_{11} & a_{12} & 0 \\ a_{21} & a_{22} & a_{23} \\ 0 & a_{32} & a_{33} \end{pmatrix}, \tag{3.2}$$

where the entries of the Jacobian V_{E_*} are

$$a_{11} = \frac{r}{1+kS_*} - 2\alpha X_* - \frac{\beta(1-m)S_*}{(1+a_1(1-m)X_*)^2},$$
$$a_{12} = -\frac{krS_*X_*}{(1+kS_*)^2} - \frac{\beta(1-m)X_*}{1+a_1(1-m)X_*},$$
$$a_{21} = \frac{\beta(1-m)S_*}{(1+a_1(1-m)X_*)^2}, \quad a_{22} = \frac{2bcI_*S_*^2}{(bS_*^2+a_2)^2}, \quad a_{23} = -\frac{cS_*}{bS_*^2+a_2},$$
$$a_{32} = \frac{-cbI_*S_*^2 + a_2cI_*}{(bS_*^2+a_2)^2},\ a_{33} = \frac{cS_*}{bS_*^2+a_2} - \delta_2.$$

The characteristic polynomial of variational matrix V_{E_*} can be written as

$$\lambda^3 + \chi_1\lambda^2 + \chi_2\lambda + \chi_3 = 0, \tag{3.3}$$

where $\chi_1 = -(a_{11}+a_{22}+a_{33})$, $\chi_2 = a_{11}a_{22} - a_{12}a_{21} + a_{22}a_{33} - a_{23}a_{32} + a_{11}a_{33}$, $\chi_3 = a_{11}a_{23}a_{32} + a_{12}a_{21}a_{33} - a_{11}a_{22}a_{33}$, $\Delta_* = -a_{11}^2(a_{22}+a_{33}) - a_{22}^2(a_{11}+a_{33}) - a_{33}^2(a_{11}+a_{22}) + a_{12}a_{21}(a_{11}+a_{22})$. According to the Routh-Hurwitz criterion, the positive equilibrium point E_* is locally asymptotically stable if $\chi_i > 0$, $i = 1, 2, 3$, and $\Delta_* > 0$ hold.

To sum up, we give the following summary.

Proposition 3.1.

- *The extinction equilibrium point $E_0 = (0, 0, 0)$ is always unstable.*
- *If $\frac{r\beta_1(1-m)}{\alpha+a_1r(1-m)} < \delta_1$ holds, the prey-only equilibrium point E_1 is locally asymptotically stable.*
- *Infected predator-free equilibrium E_2 is locally asymptotically stable if $\frac{c\bar{S}}{b\bar{S}^2+a_2} < \delta_2$, $\frac{r}{1+k\bar{S}} - 2\alpha\bar{X} - \frac{\beta(1-m)\bar{S}}{[1+a(1-m)\bar{X}]^2} < 0$.*
- *The coexistence equilibrium point E_* is locally asymptotically stable if $\chi_i > 0$, $i = 1, 2, 3$, and $\Delta_* > 0$ hold.*

3.1. Limit cycles and chaos. In this section, we mainly focus on the existence of Hopf bifurcation, limit cycle and chaos. Kolmogorov theorem [**29**] is well known to be used to solve two-dimensional (2D) prey-predator systems in theoretical biology. By changing the values of system parameters, the amplitude of periodic oscillation of the system will be changed. The Kolmogorov theorem assures that if relevant conditions are satisfied (detailed biological significance can be seen [**29**]), then there exists either stable equilibrium point or stable limit cycle behavior in the phase space of the 2D dynamical systems. Next, we discuss the conditions that satisfy the Kolmogorov theorem for different 2D systems. We start with the

susceptible predator-prey system

$$\begin{cases} \frac{\mathrm{d}X}{\mathrm{d}t} = X\left[\frac{r}{1+kS} - \alpha X - \frac{\beta(1-m)S}{1+a_1(1-m)X}\right] = XM_1, \\ \frac{\mathrm{d}S}{\mathrm{d}t} = S\left[\frac{\beta_1(1-m)X}{1+a_1(1-m)X} - \delta_1\right] = SM_2. \end{cases} \tag{3.4}$$

First, we consider the system satisfies any initial condition $X(0) > 0$, $S(0) > 0$. Then if the two-dimension system (3.4) satisfies the following conditions and requirements,

(i): $\frac{\partial M_1}{\partial X} = -\alpha + \frac{a_1\beta(1-m)^2S}{(1+a_1(1-m)X)^2} < 0$;
(ii): $X\frac{\partial M_1}{\partial X} + S\frac{\partial M_1}{\partial S} = -\frac{krS}{(1+kS)^2} - \frac{\beta(1-m)S}{(1+a_1(1-m)X)^2} - \alpha X < 0$;
(iii): $X\frac{\partial M_2}{\partial X} + S\frac{\partial M_2}{\partial S} = \frac{\beta_1(1-m)X}{(1+a_1(1-m)X)^2} > 0$;
(iv):$\frac{\partial M_2}{\partial S} = 0$;
(v): $M_1(0,0) = r > 0$;
(vi): $M_1(0,V_1) = 0 \Rightarrow V_1 = \frac{-\beta(1-m)+\sqrt{\beta^2(1-m)^2+4kr\beta(1-m)}}{2k\beta} > 0$;
(vii): $M_1(U_1,0) = 0$, $U = \frac{r}{\alpha}$;
(viii): $M_2(U_2,0)$, $U_2 = \frac{\delta_1}{(\beta_1-\delta_1a_1)(1-m)} \Rightarrow \beta_1 - \delta_1a_1 > 0$;
(ix): $\frac{r}{\alpha} > \frac{\delta_1}{(\beta_1-\delta_1a_1)(1-m)}$,

the subsystem (3.4) will produce a limit cycle or stable equilibrium point. According to [**24**], we know that the above Kolmogorov constraints can sometimes be relaxed in that an inequality can be replaced by equality.

Similarly, we consider the infected predator-prey system

$$\begin{cases} \frac{\mathrm{d}X}{\mathrm{d}t} = X\left[\frac{r}{1+kX} - \alpha X - \frac{\beta(1-m)I}{1+a_1(1-m)X}\right] = XM_1, \\ \frac{\mathrm{d}I}{\mathrm{d}t} = S\left[\frac{cX}{bS^2+a_2} - \delta_2\right] = SM_3, \end{cases} \tag{3.5}$$

we have when $\frac{r}{\alpha} > \frac{c\pm\sqrt{c^2-4a_2b\delta_2^2}}{2\delta_2 b}$, the subsystem (3.5) satisfies the K-theorem. If the above conditions are obtained, then the two-dimension system possesses either a stable equilibrium point or a stable limit cycle.

THEOREM 3.1. *The system (1.2) exhibits limit cycle or chaotic attractor, if*

$$\frac{a_1\beta(1-m)^2S}{1+a_1(1-m)X} < \alpha,\ \beta_1 > \delta_1a_1,\ \frac{r}{\alpha} > \frac{c\pm\sqrt{c^2-4a_2b\delta_2^2}}{2\delta_2 b},$$
$$\frac{-\beta(1-m)+\sqrt{\beta^2(1-m)^2+4kr\beta(1-m)}}{2k\beta} > 0$$

hold at equilibriums.

3.2. Hopf bifurcation induced by fear effect. In a population system, the change of a certain factor will destroy the stability of the system. Next, we discuss how the fear effect affects the stability of the system, we regard the fear effect as a bifurcation parameter, and investigate the Hopf bifurcation near the positive equilibrium E_*.

THEOREM 3.2. *According to [**31**], the Hopf bifurcation occurs at equilibrium E_* of system (1.2) when $k = k^*$ if the following criterion hold:*
(1): $\chi_i > 0$, $i = 1,2,3$,
(2): $\Delta_*|_{k=k^*} = 0$,
(3): $\frac{d\Delta_*}{dk}|_{k=k^*} \neq 0$, *where* χ_i *and* Δ_* *are defined in equation (3.3).*

PROOF. If $\Delta_* = 0$, then the equation (3.3) has three roots. Let $\lambda(k) = \kappa(k) + i\zeta(k)$ be the roots of (3.3) near $k = k^*$. Then we verify the following transversality condition $\frac{\mathrm{d}\Delta_*}{\mathrm{d}k}|_{k=k^*} \neq 0$, holds. putting values of $\lambda(k)$ in equation (3.3), and differentiating two sides with respect to k and separating the real and imaginary parts, ones

$$\begin{cases} F_1(k)\kappa^{'}(k) - F_2(k)\zeta^{'}(k) + F_3 = 0, \\ F_2(k)\kappa^{'}(k) + F_1(k)\zeta^{'}(k) + F_4 = 0, \end{cases} \tag{3.6}$$

where

$$F_1 = 3\kappa^2(k) + 2A_1(k)\kappa(k) + A_2(k) - 3\zeta^2(k),$$
$$F_2 = 6\kappa(k)\zeta(k) + 2A_1(k)\zeta(k),$$
$$F_3 = \kappa^2(k)A_1^{'}(k) + A_2^{'}(k)\kappa(k) + A^{'}(k) - A_1^{'}(k)\zeta^2(k),$$
$$F_4 = 2\kappa(k)\zeta(k)A_1^{'}(k) + A_2^{'}(k)\zeta(k).$$

Notice that $\kappa(k^*) = 0$, differentiating two sides of (3.3) with k, we have

$$\mathtt{Re}\left(\frac{\mathrm{d}\lambda}{\mathrm{d}k}\right)\Big|_{k=k^*} = \frac{A_3^{'}(k^*) - A_1(k^*)A_2^{'}(k^*) - A_1^{'}(k^*)A_2(k^*)}{2(A_2(k^*) + (A_1(k^*))^2)} \neq 0, \tag{3.7}$$

which means the transversality condition $\frac{\mathrm{d}\Delta_*}{\mathrm{d}k}|_{k=k^*} \neq 0$ holds.
The proof is completed. □

3.3. The stability of the bifurcating periodic solutions at $E_2(\bar{X}, \bar{S}, 0)$. This subsection discusses the stability of the bifurcating periodic solutions at the infected predator-free equilibrium $E_2(\bar{X}, \bar{S}, 0)$, for the sake of simplicity, we analyze the subsystem

$$\begin{cases} \frac{\mathrm{d}X}{\mathrm{d}t} = X\left[\frac{r}{1+kS} - \alpha X - \frac{\beta(1-m)S}{1+a_1(1-m)X}\right], & t > 0, \\ \frac{\mathrm{d}S}{\mathrm{d}t} = S\left[\frac{\beta_1(1-m)X}{1+a_1(1-m)X} - \delta_1\right], & t > 0. \end{cases} \tag{3.8}$$

Let us make a translation which is to translate E_2 to the origin by the translation $\hat{X} = X - \bar{X}$, $\hat{S} = S - \bar{S}$. For simplicity, we denote $\hat{X}$ and $\hat{S}$ by X, S, respectively, then the system (3.8) becomes

$$\begin{cases} \frac{\mathrm{d}X}{\mathrm{d}t} = (X + \bar{X})\left[\frac{r}{1 + k(S+\bar{S})} - \alpha(X + \bar{X}) - \frac{\beta(1-m)(S+\bar{S})}{1 + a_1(1-m)(X+\bar{X})}\right], \\ \frac{\mathrm{d}S}{\mathrm{d}t} = S\left[\frac{\beta_1(1-m)(X+\bar{X})}{1 + a_1(1-m)(X+\bar{X})} - \delta_1\right]. \end{cases} \tag{3.9}$$

Applying the Taylar series expansion theorem about the $(\hat{X}, \hat{S}) = (0, 0)$, and the system (3.8) can be rewritten as

$$\begin{pmatrix} \frac{\mathrm{d}X}{\mathrm{d}t} \\ \frac{\mathrm{d}S}{\mathrm{d}t} \end{pmatrix} = J\begin{pmatrix} X \\ S \end{pmatrix} + \begin{pmatrix} f(X, S, k^*) \\ g(X, S, k^*) \end{pmatrix}, \tag{3.10}$$

where,

$$J = \begin{pmatrix} \frac{r}{1+k\bar{S}} - 2\alpha\bar{X} - \frac{\beta(1-m)\bar{S}}{(1+a_1(1-m)\bar{X})^2}, & \frac{-kr\bar{X}}{(1+k\bar{S})^2} - \frac{\beta(1-m)\bar{X}}{1+a_1(1-m)\bar{X}} \\ \frac{\beta_1(1-m)\bar{S}}{(1+a_1(1-m)\bar{X})^2}, & 0 \end{pmatrix}, \tag{3.11}$$

and

$$f(X,S,k) = a_1X^2 + a_2XS + a_3S^2 + a_4X^3 + a_5X^2S + a_6XS^2 + a_7S^3,$$

$$g(X,S,k) = b_1X^2 + b_2XS + b_3S^2 + b_4X^3 + b_5X^2S + b_6XS^2 + b_7S^3$$

with

$a_1 = \dfrac{2a_1\beta(1-m)^2\bar{S}}{(1+a_1(1-m)\bar{X})^3} - 2\alpha$, $a_2 = \dfrac{-2kr}{(1+k\bar{S})^2} - \dfrac{2\beta(1-m)}{(1+a_1(1-m)\bar{X})^2}$, $a_3 = \dfrac{2k^2r\bar{X}}{(1+k\bar{S})^3}$,
$a_4 = -\dfrac{6a_1^2\beta(1-m)^3\bar{S}}{(1+a_1(1-m)\bar{X})^4}$, $a_5 = \dfrac{6a_1\beta(1-m)^2}{(1+a_1(1-m)\bar{X})^3}$, $a_6 = \dfrac{6k^2r}{(1+k\bar{S})^3}$, $a_7 = \dfrac{-6k^3r\bar{X}}{(1+k\bar{S})^4}$,
$b_1 = \dfrac{-2a_1\beta_1(1-m)^2\bar{S}}{(1+a_1(1-m)\bar{X})^3}$, $b_2 = \dfrac{\beta_1(1-m)}{(1+a_1(1-m)\bar{X})^2}$, $b_3 = 0$, $b_4 = \dfrac{6a_1\beta_1(1-m)^2}{(1+a(1-m)\bar{X})^4}$,
$b_5 = -\dfrac{2a_1^2\beta_1(1-m)^2}{(1+a(1-m)\bar{X})^3}$, $b_6 = 0$, $b_7 = 0$.

The characteristic equation of system (3.9) is

$$\iota^2 - e_1\iota + e_2e_3, \tag{3.12}$$

where

$$e_1 = \left(\frac{r}{1+k\bar{S}} - 2\alpha\bar{X} - \frac{\beta(1-m)\bar{S}}{(1+a_1(1-m)\bar{X})^2}\right),\ e_3 = \frac{\beta_1(1-m)\bar{S}}{(1+a_1(1-m)\bar{X})^2},$$
$$e_2 = \frac{-kr\bar{X}}{(1+k\bar{S})^2} - \frac{\beta(1-m)\bar{X}}{(1+a_1(1-m)\bar{X})}.$$

Define $\iota_1 = m(k)+in(k)$, $\iota_2 = m(k)-in(k)$ are the roots of (3.12) where $m(k) = \dfrac{e_1}{2}$, $n(k) = \dfrac{1}{2}\sqrt{4e_2^2e_3^2 - e_1^2}$. Next, we set a matrix

$$Q = \begin{pmatrix} N & 1 \\ M & 0 \end{pmatrix},$$

clearly,

$$Q^{-1}JQ = Q^{-1}\begin{pmatrix} e_1 & e_2 \\ e_3 & 0 \end{pmatrix}Q = J(k) = \begin{pmatrix} m(k) & -n(k) \\ n(k) & m(k) \end{pmatrix},$$

where $M = -\dfrac{e_3}{n(k)}$, $N = \dfrac{-e_1}{2n(k)}$.

By the transformation,

$$\begin{pmatrix} X \\ S \end{pmatrix} = Q\begin{pmatrix} x \\ s \end{pmatrix},$$

and the system (3.10) becomes

$$\begin{pmatrix} \dfrac{\mathrm{d}x}{\mathrm{d}t} \\ \dfrac{\mathrm{d}s}{\mathrm{d}t} \end{pmatrix} = J(k)\begin{pmatrix} x \\ s \end{pmatrix} + \begin{pmatrix} f_1(x,s,k) \\ g_1(x,s,k) \end{pmatrix}, \tag{3.13}$$

where

$$f_1(x,s,k) = \frac{1}{M}g(Nx+s, Mx, k),$$

$$g_1(x,s,k) = f(Nx+s, Mx, k) - \frac{N}{M}f_1(x,s,k).$$

Using the polar coordinate form, (3.13) becomes

$$\begin{cases} \dot{r} = r(k^*)r + a(k^*)r^3 + \ldots, \\ \dot{\theta} = \omega(k^*) + c(k^*)r^2 + \ldots. \end{cases} \tag{3.14}$$

When $k = k^*$, it follows from the Taylor expansion that

$$\begin{cases} \dot{r} = r^{'}(k^*)(k^* - k)r + a(k^*)r^3 + o\left((k^* - k)^2 r, (k^* - k)r^3, r^5\right), \\ \dot{\theta} = \omega(k^*) + \omega^{'}(k^*)(k^* - k) + c(k^*)r^2 + o\left((k^* - k)^2, (k^* - k)r^2, r^4\right). \end{cases}$$

In order to investigate the stability of Hopf bifurcation, we determine the sign of the coefficient $a(k^*)$ which is expresses as

$$\begin{aligned} a(k^*) &= \frac{1}{16}\left[F_{xxx} + F_{xss} + G_{xxs} + G_{sss}\right] \\ &\quad + \frac{1}{16\omega(k^*)}\left[F_{xs}(F_{xx} + F_{ss}) - G_{xs}(G_{xx} + G_{ss})\right. \\ &\quad \left. - F_{xx}G_{xx} + F_{ss}G_{ss}\right] |_{(0,0,k^*)}, \end{aligned} \tag{3.15}$$

where,

$$\begin{aligned} F_{xxx} &= 6\left(b_4N^2 + b_5\frac{N^3}{M}\right), \quad F_{xyy} = 2\left(\frac{3b_5}{M} + b_4\right), \quad F_{xy} = \left(\frac{2b_1N}{M} + b_2\right), \\ F_{xx} &= 2\frac{b_1N^2}{N} + b_2N, \quad F_{yy} = 2\frac{b_1}{M}, \\ G_{xxy} &= 2\left(2a_5MN + a_6M^2 + 3a_4N^2 + 3a_7N^2 - 2b_4N^2 - \frac{3b_5N^2}{M}\right), \\ G_{yyy} &= 6\left(a_4 + a_7 - \frac{b_5N}{M}\right), \quad G_{xy} = 2a_1N + a_2M - 2b_1\frac{N^2}{M} - b_2N, \\ G_{yy} &= 2\left(a_1 - \frac{b_1N}{M}\right), \quad G_{xx} = 2\left(a_1N^2 + a_2MN + a_3M^2 - b_1\frac{N^3}{M} - b_2N^2\right). \end{aligned}$$

Applying the Poincare-Andronov Hopf bifurcation theorem [**30**], we have the following conclusions:
(i): If $a(k^*) < 0$, the bifurcating periodic solution is stable and the direction of the Hopf bifurcation is subcritical;
(ii): If $a(k^*) > 0$, the bifurcating periodic solution is unstable and the direction of the Hopf bifurcation is supercritical.
By Hopf bifurcation theorem and using the formulae defined in (3.15), we can compute the corresponding values of $a_{k^*} = 13.327 > 0$ which means the bifurcating periodic solutions is unstable. According to the analysis results of E_1, E_2 and E_*, we believe that there exists the bi-stability phenomenon in system (1.2) between E_1, E_* and a limit cycle, see Fig. 1.

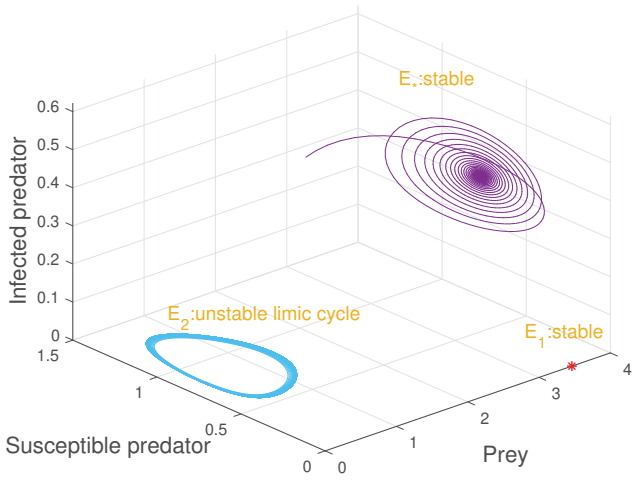

Fig. 1. Phase portrait for system (1.2), the stability around E_1, E_2 and E_*, respectively, all parameters are set in Table 1, except $k = 0.25$, $k = 0.6$, $k = 2$ respectively.

For cases beyond the scope of analytical methods, in order to explore the complex dynamics of the system (1.2), we use numerical simulation to verify the conclusions. We choose an arbitrary set of stable coexistence equilibrium $E_* = (1.1188, 0.3770, 0.1004)$. In Fig. 2, we present E_* is stable with three different initial value, they eventually balance out to a common point. We verify that the Routh-Hurwitz stability criterions automatically hold by calculating, including $A_1 = 0.2006 > 0$, $A_2 = 0.0257 > 0$, $A_3 = 0.0056 > 0$, $A_1A_2 - A_3 = 0.0184 > 0$, the parameters are in Table 1. We perform extensive simulations to observe the dynamical behavior of the deterministic system (1.2). In Fig. 3, we see the coexistence equilibrium E_* losses its stability and a Hopf-bifurcation occurs at the critical value $k^* = 0.173$. When $k > k^*$, E_* becomes stable. We control the parameter k in [0, 0.45] and observe the influence of parameter changes on system stability, as shown in Fig. 3, bifurcation diagrams are generated for the population densities of prey, susceptible and infected predators, respectively. The E_* is stable for $k > 0.173$ and losses its stability for $k < 0.173$. And critical Hopf bifurcation occurs at $k = 0.173$. In Fig. 4, the three species population oscillates in a range, and a stable limit cycle emerges when $k = 0.1$. As the value of k increases to 0.6, a stable focus attractor appears and the impact of time variation on the population density of species is presented. The 3D view of the limit cycle and the stable focus point is presented in Fig. 5. When k is large, such as $k = 2$, the infected predator goes to extinct, it tends to the equilibrium E_2 instead of E_*, we can see Fig. 6. Too large value of k can reduce the number of species. Fig. 7 is the 3D view.

The birth rate r of prey shows quite complex population dynamic behaviors. In Fig. 8a, we present a chaotic attractor when $r = 1.45$ and all other values are fixed in Table 1. Fig. 8b is the phases of time evolution. Attractors set in x-y-view for $r = 0.2$, $r = 0.6$, and $r = 1.5$, respectively are presented in Fig. 9. We made a comparison by changing the values of the fear effect k and the values of the prey

refuge m, The prey refuge can promote the stability of the system. In Fig. 10a to Fig. 10c, we fix $k = 0.55$, and choose $m = 0$, $m = 0.5$, $m = 0.9$ respectively, the stability of E_* is not change with different m. From the perspective of population density, with the increase of m, the population density of prey increases, but on the contrary, the density of predators decreases. When the protection force is large, the infected predator becomes extinct. On the other hand, from Fig. 10d to Fig. 10f, we can verify that k can change the stability of the system once by changing the values of k and fixing $m = 0.25$. At the same time, we discuss the defensive ability of susceptible predators, it is observed that the defense efficiency of the susceptible predator has a significant role in the population dynamics, it can not change the stability of coexisting equilibrium E_*, but it has a strong negative effect on the prey population and infected population. Biologically, it suggests that the better defense of the susceptible predator reduces the ability of the infected predator to infect, resulting in stronger predation on prey and lower growth of the infected predator, which can be reflected in Fig. 11.

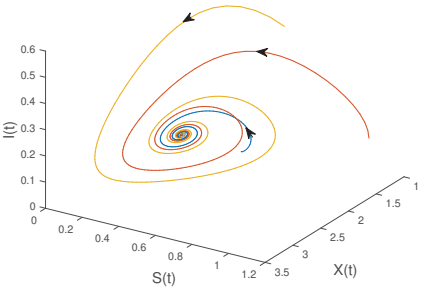

Fig. 2. Phase portrait for system (1.2), E_* is globally asymptotically stable with different initial values.

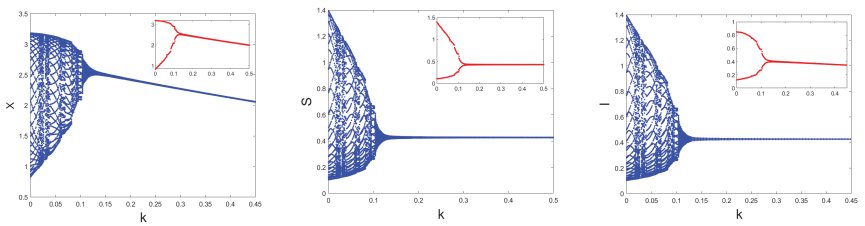

Fig. 3. Bifurcation diagram for level of fear effect k, and other parameter values are given in Table 1. (a) Prey population, (b) Susceptible predator population, (c) Infected predator population.

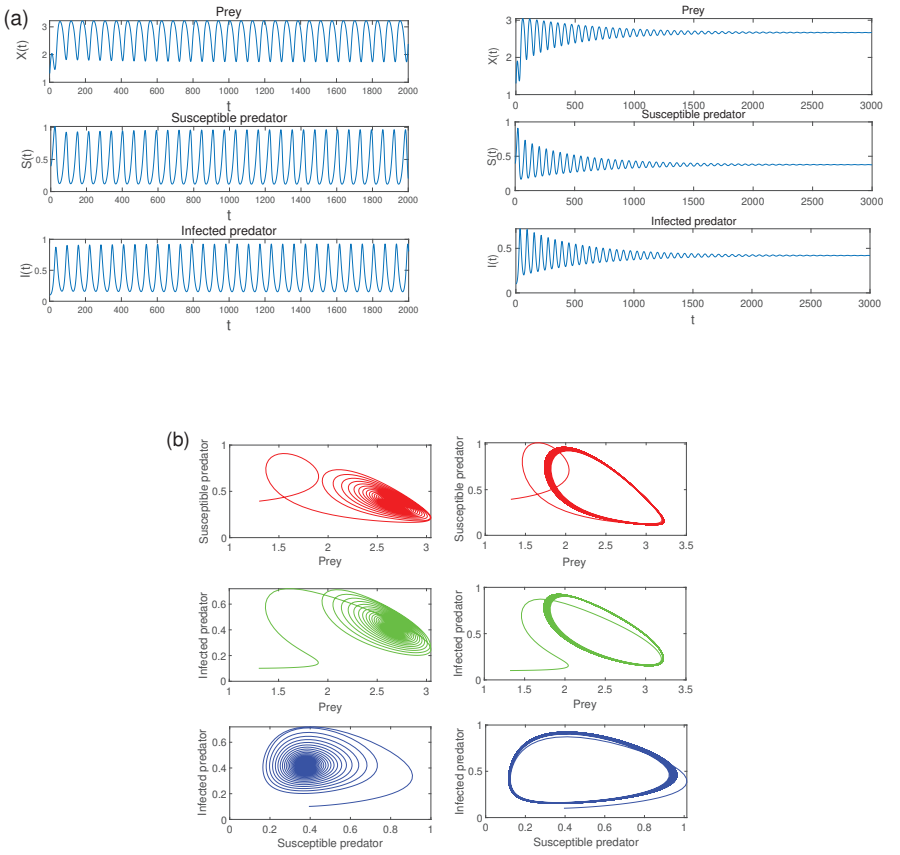

Fig. 4. (a): Time-series plots for prey, susceptible predator, infected predator. Left figure is $k = 0.1$, right figure is $k = 0.6$. (b): Phase diagrams of system (1.2) when $k = 0.1$ and $k = 0.6$, other parameters are fixed.

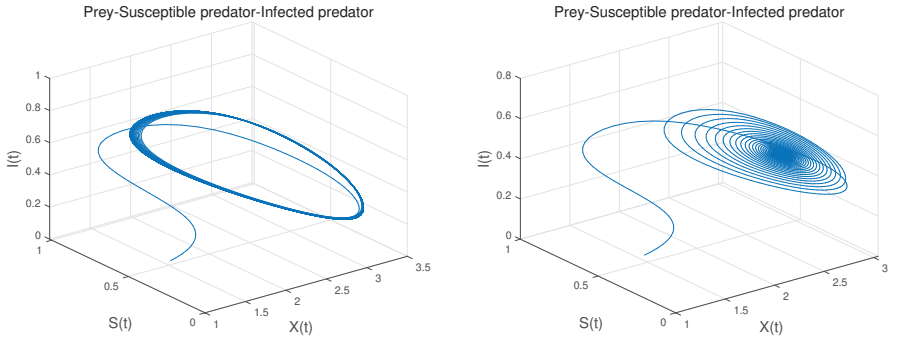

Fig. 5. 3D view of stable focus for prey-susceptible predator-infected predator when $k = 0.1$ and $k = 0.6$.

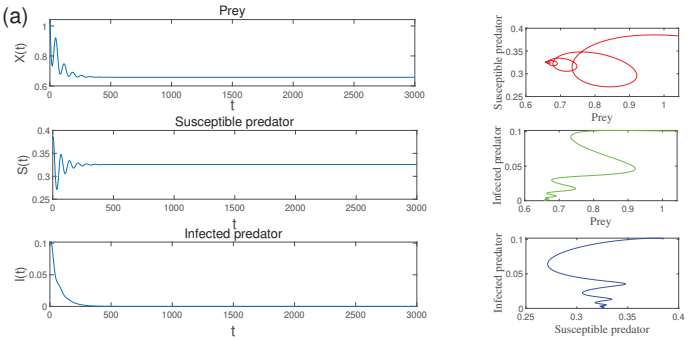

Fig. 6. (a): Time-series plots for prey, susceptible predator and infected predator. (b): Phase diagram of system (1.2) when $k = 2$ and other parameters are fixed.

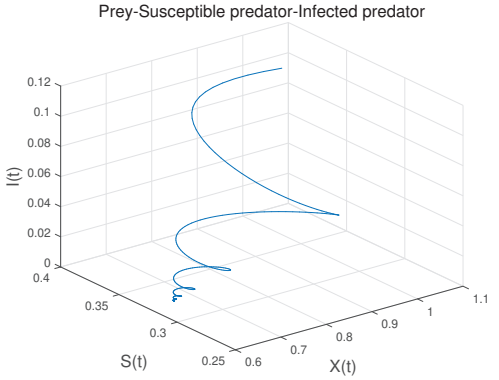

Fig. 7. 3D view of infected predator-free for prey-susceptible predator-infected predator when $m = 0.85$, $k = 0.1$.

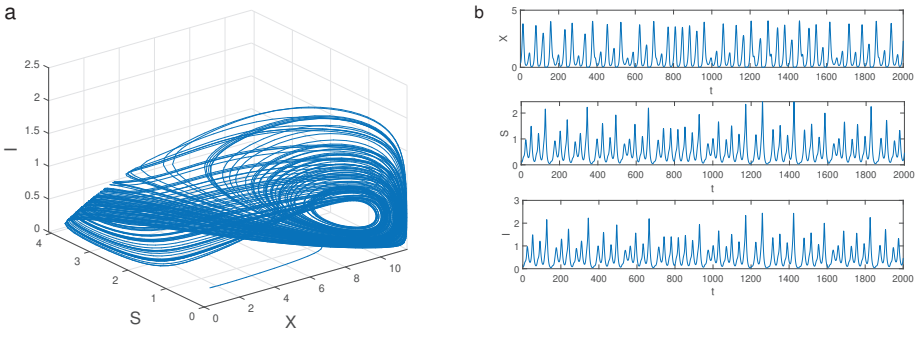

Fig. 8. (a): The chaotic attractor of system (1.2). (b): Time-domain waves for $X(t)$, $S(t)$, and $I(t)$ of system (1.2).

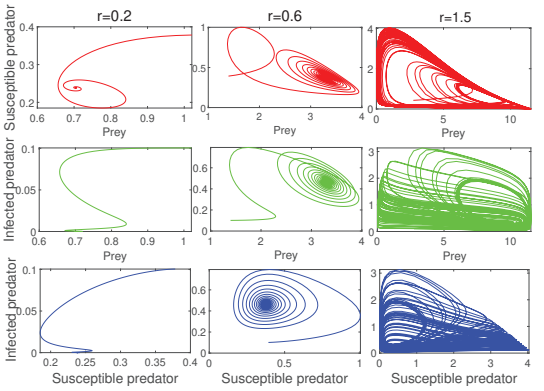

Fig. 9. Attractors set in x-y-view for different value of r and keeping other parameters fixed as in Table 1: $r = 0.2$, $r = 0.6$, $r = 1.5$, respectively.

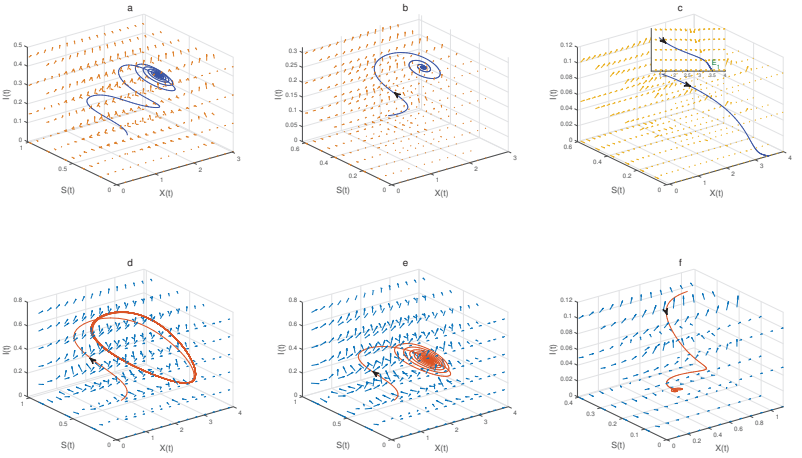

Fig. 10. Phase portraits of system (1.2) with other parameters set in Table 1 except (a) m = 0, k = 0.55; (b) m = 0.5, k = 0.55; (c) m = 0.9, k = 0.55; (d) m = 0.25, k = 0.05; (e) m = 0.25, k = 0.25; (f) m = 0.25, k = 0.9.

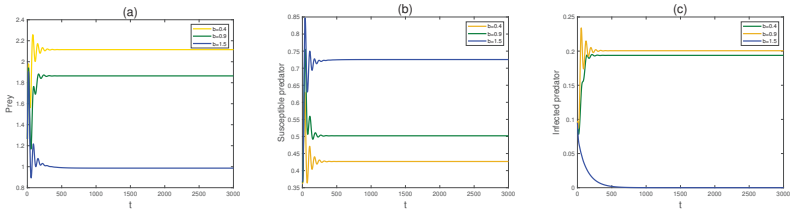

Fig. 11. Time series of prey, susceptible predator and infected predator for system (1.2) corresponding with b.

4. Properties of diffusion induced system

In this section, we discuss the local stability and Turing instability of spatial diffusion system, we give the conditions of local stability and diffusion-driven equilibrium instability. Firstly, we obtain the local stability conditions of the spacial diffusion system, and then prove that the spacial diffusion can make the uniform steady state be unstable, and hence leads to the Turing instability.

4.1. Local stability. For the convenience of discussion, the linearization of the system (1.3) at the homogeneous steady state $E_*(X_*, S_*, I_*)$ can be expressed by

$$\begin{pmatrix} \dfrac{\partial X(x,t)}{\partial t} \\ \dfrac{\partial S(x,t)}{\partial t} \\ \dfrac{\partial I(x,t)}{\partial t} \end{pmatrix} = D\triangle \begin{pmatrix} X(x,t) \\ S(x,t) \\ I(x,t) \end{pmatrix} + A_0 \begin{pmatrix} X(x,t) \\ S(x,t) \\ I(x,t) \end{pmatrix}, \tag{4.1}$$

where

$$D = \begin{pmatrix} d_1 & 0 & 0 \\ 0 & d_2 & 0 \\ 0 & 0 & d_3 \end{pmatrix}, \qquad A_0 = \begin{pmatrix} a_{11} & a_{12} & a_{13} \\ a_{21} & a_{22} & a_{23} \\ a_{31} & a_{32} & a_{33} \end{pmatrix},$$

A_0 has the same meaning with (3.2). The corresponding Jacobian matrix of (4.1) at E_* is

$$J_2 = \begin{pmatrix} d_1\Delta + a_{11} & a_{12} & a_{13} \\ a_{21} & d_2\Delta + a_{22} & a_{23} \\ a_{31} & a_{32} & d_3\Delta + a_{33} \end{pmatrix}.$$

Let μ_l is an eigenvalue of J_2, we have the matrix

$$W = \begin{pmatrix} -d_1\mu_l + a_{11} & a_{12} & a_{13} \\ a_{21} & -d_2\mu_l + a_{22} & a_{23} \\ a_{31} & a_{32} & -d_3\mu_l + a_{33} \end{pmatrix}. \tag{4.2}$$

From the (4.2), we can get the characteristic polynomial

$$\mu_l^3 + \Phi_1(l)\mu_l^2 + \Phi_2(l)\mu_l + \Phi_3 = \Delta_l,\ l \in \mathbb{N}_0, \tag{4.3}$$

where

$$\begin{aligned}
\Phi_1(l) &= (d_1 + d_2 + d_3)l + \chi_1, \\
\Phi_2(l) &= (d_1d_2 + d_1d_3 + d_2d_3)l^2 - ((a_{22} + a_{33})d_1 + (a_{11} + a_{33})d_2 \\
&\quad +(a_{11} + a_{22})d_3)\, l + \chi_2, \\
\Phi_3(l) &= d_1d_2d_3l^3 - (d_1d_3a_{22} + d_2d_3a_{11})l^2 + (d_1(a_{22}a_{33} - a_{23}a_{32}) + d_2a_{11}a_{33} \\
&\quad + d_3(a_{11}a_{22} - a_{12}a_{21}))l + \chi_3,
\end{aligned}$$

χ_1, χ_2, and χ_3 have the same meanings with the equation (3.3).

THEOREM 4.1. *Assuming $\chi_i > 0$, $i = 1, 2, 3$, and $\Delta_* > 0$ always hold. According to to Routh-Hurwitz criterion, we can confirm the spacial diffusion system (4.1) is local stable around the coexistence equilibrium steady state E_* when the following conditions hold:*
(1): $\Phi_1(l) > 0$;
(2): $\Phi_2(l) > 0$;

(3): $\Phi_3(l) > 0$;
(4): $\Delta_\Phi = \Phi_1(l)\Phi_2(l) - \Phi_3(l) > 0$.

PROOF. It is clearly that $\Phi_1(l) > 0$ always holds. For $\Phi_2(l)$, we consider the quadratic equation of one variable, when $(a_{22}+a_{33})d_1+(a_{11}+a_{33})d_2+(a_{11}+a_{22})d_3 < 0$, then $\Phi_2(l) > 0$ holds. Define

$$\Delta_\Phi = \Phi_1(l)\Phi_2(l) - \Phi_3(l) = \Upsilon_1 l^3 + \Upsilon_2 l^2 + \Upsilon_3 l + \Upsilon, \tag{4.4}$$

where

$$\begin{aligned}
\Upsilon_1 &= (d_1 + d_2 + d_3)(d_1d_2 + d_2d_3 + d_1d_3) - d_1d_2d_3,\\
\Upsilon_2 &= -(a_{11} + a_{22})(d_1d_2 + d_3(d_1 + d_2 + d_3))\\
&\quad - (a_{22} + a_{33})(d_2d_3 + d_1(d_1 + d_2 + d_3)) - (a_{11} + a_{33})(d_1d_3 + d_2(d_1 + d_2 + d_3)),\\
\Upsilon_3 &= (d_1 + d_2 + d_3)\chi_2 - [(a_{22} + a_{33})d_1 + (a_{11} + a_{22})d_3 + (a_{11} + a_{33})d_2]\,\chi_1\\
&\quad - [d_1(a_{22}a_{33} - a_{23}a_{32}) + d_2a_{11}a_{33} + d_3(a_{11}a_{22} - a_{12}a_{21})]\,,\\
\Upsilon &= -(a_{11} + a_{22} + a_{33})(a_{11}a_{22} + a_{22}a_{33} + a_{11}a_{33} - a_{23}a_{32} - a_{12}a_{21})\\
&\quad + (a_{11}a_{22}a_{33} - a_{12}a_{21}a_{33} - a_{11}a_{23}a_{32}).
\end{aligned}$$

Thus we basically get the stability property. □

Below we discuss how the spatial diffusion affects the stability of the system in a predator-prey system with diffusion.

4.2. Hopf bifurcation for system (1.3) near E_*. In this subsection, applying Hopf bifurcation theorem [**33**], we investigate the bifurcation solution of the system(1.3) near E_* by taking r as a bifurcation parameter.

THEOREM 4.2. *Hopf bifurcation occurs at $r = r^*$ for the reaction-diffusion system (1.3), if* $\dfrac{d\Delta_\Phi}{dr}\,|_{r=r^*} \neq 0$.

PROOF. Indeed, solving the roots of a cubic equation with one variable is more complicated, we assume that there exists one root with a negative real part and the other two roots are pure imaginary roots which are $-\theta$, ηi and $-\eta i$. The characteristic equation can be expressed as

$$(\mu_l + \theta)(\mu_l + \eta i)(\mu_l - \eta i) = 0,$$

by a simple calculation, we have

$$\mu_l^3 + \theta\mu_l^2 + \eta^2\mu_l + \theta\eta^2 = 0, \tag{4.5}$$

compared with equation (4.3), we obtain

$$\theta = \Phi_1(l), \quad \eta^2 = \Phi_2(l), \quad \theta\eta^2 = \Phi_3.$$

It is obviously that $\Delta_\Phi = \Phi_1\Phi_2 - \Phi_3 = 0$.

Let l be a positive constant, differentiating with respect to r, similar to Theorem 3.2, one yields

$$\frac{\mathrm{d}\Delta_\Phi}{\mathrm{d}r}\,|_{r=r^*} \neq 0.$$

According to [**32**], Hopf bifurcation occurs in the reaction-diffusion system (1.3) near the E_*. This bifurcation solution is spatially dependent and the bifurcation is induced by diffusion.
The proof is completed. □

4.3. Diffusion induced instability. In nature, the population system is always affected by spatial factors, and the system instability caused by spatial diffusion is called Turing instability. In this subsection, we discuss the conditions that lead to Turing instability. Assume that $\chi_1 > 0$, $\chi_2 > 0$, $\chi_3 > 0$, $\Delta_* > 0$. If any one of the Theorem (4.1) does not hold, then the Turing instability may occur. Obviously, $\Phi_1(l) > 0$ always holds, then we analyze $\Phi_2(l)$, $\Phi_3(l)$ and Δ_Φ.
(1) For

$$\begin{aligned}\Phi_2(l) &= (d_1d_2 + d_1d_3 + d_2d_3)l^2 \\ &\quad - ((a_{22} + a_{33})d_1 + (a_{11} + a_{33})d_2 + (a_{11} + a_{22})d_3)\, l + \chi_2 > 0,\end{aligned}$$

which implies that the polynomial must have two positive roots

$$l_1 = \frac{-\varrho + \sqrt{\varrho^2 - 4\varpi\varsigma}}{2\varsigma} \text{ and } l_2 = \frac{-\varrho - \sqrt{\varrho^2 - 4\varpi\varsigma}}{2\varsigma},$$

where

$$\varrho = (a_{22} + a_{33})d_1 + (a_{11} + a_{33})d_2 + (a_{11} + a_{22})d_3,$$
$$\varsigma = d_1d_2 + d_1d_3 + d_2d_3, \quad \varpi = \chi_2.$$

Consequently, we obtain the following conclusions that Turing instability is possible:
(i) $\Phi_2(l) < 0, \quad if \quad l_1 < 0$,
(ii) $\varrho^2 - 4\varpi\varsigma > 0$.
(2) For

$$\begin{aligned}\Phi_3(l) &= d_1d_2d_3l^3 - (d_1d_3a_{22} + d_2d_3a_{11})l^2 \\ &\quad + (d_1(a_{22}a_{33} - a_{23}a_{32}) + d_2a_{11}a_{33} + d_3(a_{11}a_{22} - a_{12}a_{21}))l + \chi_3,\end{aligned} \tag{4.6}$$

for convenience, define

$$\psi_1 = d_1d_2d_3, \quad \psi_2 = d_1d_3a_{22} + d_2d_3a_{11},$$
$$\psi_3 = d_1(a_{22}a_{33} - a_{23}a_{32}) + d_2a_{11}a_{33} + d_3(a_{11}a_{22} - a_{12}a_{21}),$$

differentiating the equation (4.6) with respect to l, yields

$$\Phi_3^{'}(l) = 3\psi_1l^2 - 2\psi_2l + \psi_3, \tag{4.7}$$

the equation (4.7) has two extreme points

$$l_{\min} = \frac{-\psi_2 + \sqrt{4\psi_2^2 - 12\psi_1\psi_3}}{6\psi_1}, \quad l_{\max} = \frac{-\psi_2 - \sqrt{4\psi_2^2 - 12\psi_1\psi_3}}{6\psi_1}.$$

Hence, Turing instability may occurs if
(i) $4\psi_2^2 - 12\psi_1\psi_3 > 0$,
(ii) $\Phi_3(l) < 0, \quad if \quad l_{min} < 0$.
Taking advantage of the same way, we can obtain the relevant conclusions for $\Delta_\Phi < 0$.

5. Numerical simulations for reaction-diffusion system

We present some numerical simulations to study the dynamic of the eco-epidemiological system as well as to verify and supplement the numerical results given in the previous sections. In addition, we study the effects of fear effect and prey refuge on the dynamics of the populations and give their biological significance. In the non-space system and the reaction-diffusion system, we give the correlation figures of the influence of parameter changes on the system stability. The parameters are given in Table 1. Next, we conduct numerical simulations from diffusion d_1,

d_2, d_3 and r, respectively. For the solution initiated from $X(x,0) = 1.1188 + 0.1\sin(0.5x)$, $S(x,0) = 0.3770 + 0.1\sin(0.5x)$, $I(x,0) = 0.4766 + 0.1\sin(0.5x)$.

For the stable focus point around E_* of system (1.2) with $d_1 = d_2 = d_3 = 0$ (see Fig. 2), in Fig. 12, we choose small values for diffusion coefficients with $d_1 = 0.01$, $d_2 = 0.001$, and $d_3 = 0.0001$, which also satisfies Routh-Hurwitz criterions: $\chi_1 = 0.1904 > 0$, $\chi_2 = 0.0257 > 0$, $\chi_3 = 0.0001004 > 0$, $\Delta_* = \chi_1\chi_2 - \chi_3 = 0.0186 > 0$, the system (1.3) is stable, while Fig. 13 shows that for a large value for $d_1 = 1$, a spatial periodic solution appears with $\chi_2 = -0.00001$, $\chi_3 = -0.0047$, $\chi_1\chi_2 - \chi_3 = -0.0094$. For the effect of diffusion parameter d_3, when we increase d_3 to 0.001, we can see in Fig. 14 that the solution converges to E_2, which implies that a large d_3 may make the infected predator go extinct, and it promotes the stability of the reaction-diffusion system (2.1). When $r > r^*$, the system (1.3) occurs Hopf instability, we can see in Fig. 15. Fig. 16 represents the bifurcation diagrams generated for the successive maxima of the population densities S, X and I in the ranges $[0.0, 12]$, $[0.0, 4.5]$ and $[0.0, 2.5]$ respectively for r which is in the range of $[0.2, 1.45]$ and the other parameters are fixed in Table. 1. From Fig. 17a, d_1 can promote the occurrence of Turing instability, while d_2 can inhibit the occurrence of Turing instability in Fig. 19b. blue color is for spatial system when $d_1 = 0.1$, $d_2 = 0.1$, $d_3 = 0.001$ and red color is for the non-spatial system. Fig. 17c is the comparison of the bifurcation appearing around the coexistence steady state E_* for the non-spatial system and the spatial system with respect to r, it can be observed that in the spatial system, bifurcation occurs earlier than it in the deterministic system. Moreover, we give the space plot of the spacial system (1.3) at $r = 0.9$ and $r = 1.5$. When $r = 0.9$, there exists periodic phenomenon in the space, as r increases to 1.5, the space trajectory becomes chaotic.

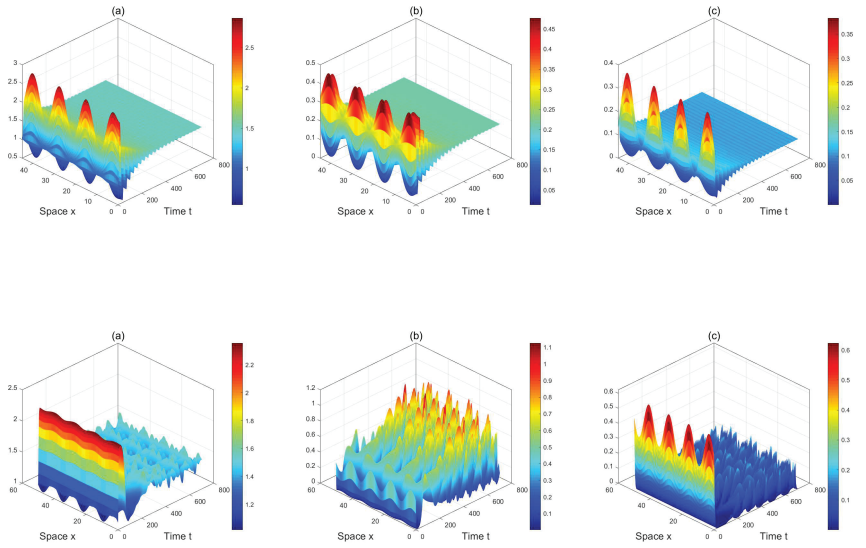

Fig. 12. Plots of system (4.1) with $d_1 = 0.1$, $d_2 = 0.001$, $d_3 = 0.0001$ in the first line, $d_1 = 1$, $d_2 = 0.001$, $d_3 = 0.0001$ in the second line (a), (a'): prey, (b), (b'): susceptible predator, (c), (c'): infected predator.

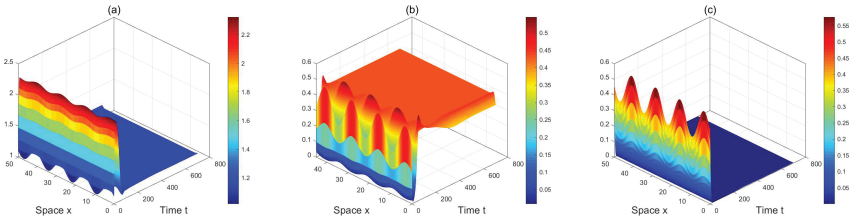

Fig. 13. Plots of system (4.1) with $d_1 = 1$, $d_2 = 0.001$, $d_3 = 0.001$, (a): prey, (b): susceptible predator, (c): infected predator.

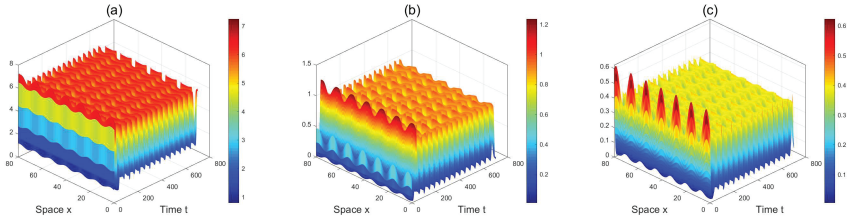

Fig. 14. Plots of system (4.1) with $d_1 = 0.1$, $d_2 = 0.001$, $d_3 = 0.001$, $r = 0.9$ (a): prey, (b): susceptible predator, (c): infected predator.

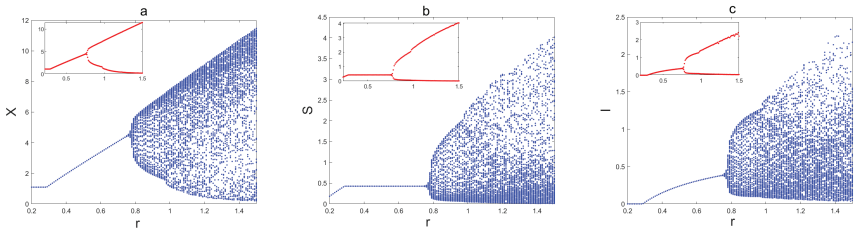

Fig. 15. Bifurcation diagram for intrinsic growth rate r, and other parameter values are given in Table 1. (a) Prey, (b) Susceptible predator, (c) Infected predator.

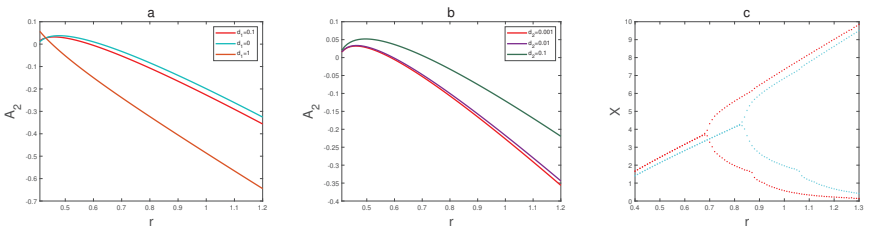

Fig. 16. a: the curves of A_2 and d_1, b: the curves of A_2 and d_2 when $r \in [0.4 - 1.2]$, c: bifurcation diagram for prey with intrinsic growth rate r.

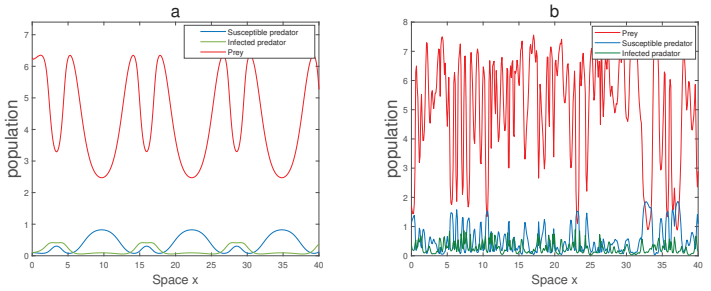

Fig. 17. Numerical solution of the space plot for system (1.3), a: $r = 0.9$, b: $r = 1.45$.

6. Conclusion

In nature, the predation relationship between prey and predator is the most basic one. Due to predator hunting, prey may produce the fear effect and take protective measures against such hunting. Infectious diseases are highly essential factors affecting the size of human and animal populations. The infectious diseases and predator-prey interactions produce complex effects that regulate predator and prey densities. As an illustration of these common phenomenons, in this paper, we propose a reaction-diffusion eco-epidemiological system with two-predator-one-prey that considers fear effect and prey refuge. We prove that positive solutions exist and are bounded, and obtain the existence conditions of all equilibrium points in biological significance, and study the stability of system (1.2) at different equilibrium points by using the Jacobian matrix.

We would also like to mention that the fear effect k can induce Hopf bifurcation, we regard the fear effect k as a bifurcation parameter, and we verify the existence of Hopf bifurcation in the deterministic system (1.2) at the critical point k^*. Moreover, we find that when the degree of the fear effect is too large, the number of both prey and predator will decrease, but when the fear effect is too small, the system will be unstable. At the same time, it is found by numerical simulation that when the growth coefficient r of prey exceeds a threshold value, the coexistence population state may be unstable. When the growth rate of the prey is particularly slow, the density of diseased predators tends to zero. Moreover, we studied the influence of prey refuge on the system stability. We found that the change of prey refuge can not make the stable system become unstable, but the increase of prey refuge value m would make the unstable system become stable. However, when the refuge value m is too high, it can lead to a decrease in population density and may lead to the extinction of predators. We conduct numerical simulation on the protection coefficient b of the susceptible predator, and find that when the b is higher, the density of both prey and infected predators may decrease, and on the contrary, the density of the susceptible predator increases.

When we consider the influence of spatial diffusion on the system, we find that diffusion instability will appear when the prey diffusion is more active and the propagation speed is relatively fast. We derive conditions for Turing instability and examine the consequences of defense and cannibalism in pattern formation. We used numerical simulation to explore the following characteristics: when we fix the other parameters, and change the diffusion parameters d_1 and d_2, from

the figures, unlike the case of classical linear diffusion, the Turing instability can be suppressed when diffusion of the d_2 become fast while d_1 can promote the occurrence of Turing instability. Moreover, spatial diffusion can lead to an earlier occurrence of bifurcation.

Our research suggests that understanding the dynamics of ecosystems with the infectious diseases can help us better facilitate the evolution of biological systems. The defense effect of the prey, fear effect and the defense effect of susceptible predator on infected predator all affect population stability and population density change. In addition, controlling the birth rate of the prey is also important for the stability of the system. It is an important task to consider the optimal harvest of species in the fishing industry and fishing industry. In the future research, we will combine economic benefits to establish a model and get the optimal harvest scheme, we will also study spatial instability due to time delay, such as [**34**] and so on.

Acknowledgements

This work was supported by the Research Fund for the Taishan Scholar Project of Shandong Province of China, Shandong Provincial Natural Science Foundation of China (ZR2019MA003), the SDUST Innovation Fund for Graduate Students (YC20210217).

References

[1] C.J. Wei, L.S. Chen, Eco-epidemiology model with age structure and prey-dependent consumption for pest management, Appl. Math. Model. **33** (2009), 4354-4363.
[2] X.Y. Liang, Y.Z. Pei, M.X. Zhu, Y.F. Lv, Multiple kinds of optimal impulse control strategies on plant-pest-predator model with eco-epidemiology, Appl. Math. Comput. **277-278** (2016), 1-11.
[3] M. Su, C. Hui, Y.Y. Zhang, Z.Z. Li, Spatiotemporal dynamics of the epidemic transmission in a predator-prey system, B. Math. Biol. **70** (2008), 2195-2210.
[4] H.X. Hu, L.G. Xu, K. Wang. A comparison of deterministic and stochastic predator-prey models with disease in the predator, Discrete Cont. Dyn-B. **24(6)** (2019), 2837-2863.
[5] S.K. Sasmal, Y. Takeuchi, Modeling the Allee effects induced by cost of predation fear and its carry-over effects, J. Math. Anal. Apll. **505** (2022), 125485.
[6] T. Feng, X.Z. Meng, L.D. Liu, S.J. Gao, Application of inequalities technique to dynamics analysis of a stochastic eco-epidemiology model, J. Inequal. Appl. **327** (2016).
[7] X.B. Zhang, Q. An, L. Wang, Spatiotemporal dynamics of a delayed diffusive ratio-dependent predator-prey model with fear effect, Nonlinear Dynam. **105** (2021), 3775-3790.
[8] P. Panday, N. Pal, S. Samanta, J. Chattopadhyay, Stability and Bifurcation Analysis of a Three-Species Food Chain Model with Fear, Int. J. Bifurcat. Chaos **28** (2018), 1850009.
[9] H.K. Qi, X.Z. Meng, Threshold behavior of a stochastic predator-prey system with prey refuge and fear effect, Appl. Math. Lett. **113** (2021), 106846.
[10] V. Tiwari, J.P. Tripathi, S. Mishra, R.K. Upadhyay, Modeling the fear effect and stability of non-equilibrium patterns in mutually interfering predator-prey systems, Appl. Math. Comput. **371** (2020), 124948.
[11] X.Y. Wang, L. Zanette, X.F. Zou, Modelling the fear effect in predator-prey interactions, J. Math. Biol. **73** (2016), 1179-1204.
[12] R. Banerjee, P. Das, D. Mukherjee, Effects of fear and anti-predator response in a discrete system with delay, Discrete Cont. Dyn-B. (2021).
[13] S.Q. Zhang, S.L. Yuan, T.H. Zhang, A predator-prey model with different response functions to juvenile and adult prey in deterministic and stochastic environments, Appl. Math. Comput. **413(15)** (2022), 126598.
[14] H.W. Hethcote, W.D. Wang, L.T. Han, Z.E. Ma, A predator-prey model with infected prey, Theor. Popul. Biol. **66** (2004), 259-268.
[15] P. KumarKar, Stability analysis of a prey-predator model incorporating a prey refuge, Commun Nonlinear Sci. **10(6)** (2005), 681-691.

[16] X.L. Sun, R. Yuan, Hopf bifurcation in a diffusive population system with nonlocal delay effect, Nonlinear Anal. **214** (2022), 112544.
[17] J. Ghosh, B. Sahoo, S. Poria, Prey-predator dynamics with prey refuge providing additional food to predator, Chaos Soliton. Fract. **96** (2017), 110-119.
[18] N. Sk, P.K. Tiwari, S. Pal, A delay nonautonomous model for the impacts of fear and refuge in a three species food chain model with hunting cooperation, Math. Comput. Simulat. **192** (2022), 136-166.
[19] M. Moustafa, M.H. Mohd, A.I. Ismail, F.A. Abdullah, Dynamical analysis of a fractional order eco-epidemiological model with nonlinear incidence rate and prey refuge, J. Appl. Math. Comput. **65** (2021), 623-650.
[20] T.K. Kar, Modelling and analysis of a harvested prey-predator system incorporating a prey refuge, J. Comput. Appl. Math. **185** (2006), 19-33.
[21] J.B. Collings, Bifurcation and stability analysis of a temperature-dependent mite predator-prey interaction model incorporating a prey refuge, B. Math. Biol. **57** (1995), 63-76.
[22] L.L. Ji, C.Q. Wu, Qualitative analysis of a predator-prey model with constant-rate prey harvesting incorporating a constant prey refuge, Nonlinear Anal-Real. **11(4)** (2010), 2285-2295.
[23] CS. Holling, The functional response of predators to prey density and its role in mimicry and population regulation, Mem Entomolog Soc Can. **45** (1965), 5-60.
[24] S.N. Rawa, P. Mishraa, R. Kumar, S. Thakur, Complex behavior of prey-predator system exhibiting group defense: A mathematical modeling study, Chaos Soliton, Fract. **100** (2017), 74-90.
[25] H.S. Zhang, Y.L. Cai, S.M. Fu, W.M. Wang, Impact of the fear effect in a prey-predator model incorporating a prey refuge, Appl. Math. Comput. **356** (2019), 328-337.
[26] P. Mishra, S.N. Raw, B. Tiwari, On a cannibalistic predator-prey model with prey defense and diffusion, Appl. Math. Model. **90** (2021), 165-190.
[27] X.Z. Meng, F. Li, S.J. Gao, Global analysis and numerical simulations of a novel stochastic eco-epidemiological model with time delay, Appl. Math. Comput. **339** (2018), 701-726.
[28] B. Chakraborty, N. Bairagi, Complexity in a prey-predator model with prey refuge and diffusion, Ecol. Complex. **37** (2019), 11-23.
[29] R.M. May, Stability and Complexity in Model Ecosystems, Princeton, NJ: Princeton University Press; 2001.
[30] J. E. Marsden, M. McCracken, The Hopf Bifurcation and Its Applications, Springer-Verlag New York (1976).
[31] W.M. Liu, Criterion of hopf bifurcations without using eigenvalues, J. Math. Anal. Appl. **182** (1994), 250-256.
[32] Y.F. Jia, Y. Li, J.H. Wu, Effect of predator cannibalism and prey growth on the dynamic behavior for a predator-stage structured population model with diffusion, J. Math. Anal. Appl. **449** (2017), 1479-1501.
[33] Hassard, B.D., Kazarinoff, N.D., Wan, Y.H., Theory and Applications of Hopf Bifurcation, Cambridge Univ. Press, Cambridge, 1981.
[34] Y.L. Song, Y. Peng, T.H. Zhang, The spatially inhomogeneous Hopf bifurcation induced by memory delay in a memory-based diffusion system, J. Differ. Equ. **300** (2021), 597-624.

College of Mathematics and Systems Science, Shandong University of Science and Technology Qingdao 266590, PR China
Email address: mxz721106@sdust.edu.cn